

Productivity and phenological responses of natural vegetation to present and future inter-annual climate variability across semi-arid river basins in Chile

Francisco E. Glade · Marcelo D. Miranda ·
Francisco J. Meza · Willem J. D. van Leeuwen

Received: 5 May 2016 / Accepted: 31 October 2016 / Published online: 17 November 2016
© Springer International Publishing Switzerland 2016

Abstract Time series of vegetation indices and remotely sensed phenological data offer insights about the patterns in vegetation dynamics. Both are useful sources of information for analyzing and monitoring ecosystem responses to environmental variations caused by natural and anthropogenic drivers. In the semi-arid region of Chile, climate variability and recent severe droughts in addition to land-use changes pose threats to the stability of local ecosystems. Normalized difference vegetation index time series (2000–2013) data from the moderate resolution imaging spectroradiometer (MODIS) was processed to monitor the trends and patterns of

vegetation productivity and phenology observed over the last decade. An analysis of the relationship between (i) vegetation productivity and (ii) precipitation and temperature data for representative natural land-use cover classes was made. Using these data and ground measurements, productivity estimates were projected for two climate change scenarios (RCP2.6 and RCP8.5) at two altitudinal levels. Results showed negative trends of vegetation productivity below 2000 m a.s.l. and positive trends for higher elevations. Phenology analysis suggested that mountainous ecosystems were starting their growing period earlier in the season, coinciding with a decreased productivity peak during the growing season. The coastal shrubland/grassland land cover class had a significant positive relation with rainfall and a significant negative relation with temperature, suggesting that these ecosystems are vulnerable to climate change. Future productivity projections indicate that under an RCP8.5 climate change scenario, productivity could decline by 12% in the period of 2060–2100, leading to a severe vegetation degradation at lower altitudes and in drier areas.

F. E. Glade · M. D. Miranda · F. J. Meza
Department of Ecosystem and Environment, Pontificia
Universidad Católica de Chile, Av. Vicuña Mackenna 4860,
7820436 Santiago, Chile

M. D. Miranda (✉)
Center of Applied Ecology & Sustainability (CAPES), Pontificia
Universidad Católica de Chile, Santiago, Chile
e-mail: mmirands@uc.cl

F. J. Meza
Centro Interdisciplinario de Cambio Global, Pontificia
Universidad Católica de Chile, Santiago, Chile

W. J. D. van Leeuwen
School of Natural Resources and the Environment, Office of Arid
Lands Studies, Arizona Remote Sensing Center, The University of
Arizona, 1955 E. Sixth Street, Tucson, AZ 85721, USA

W. J. D. van Leeuwen
School of Geography and Development, The University of
Arizona, Tucson, AZ 85721, USA

Keywords Vegetation productivity · Phenology trends ·
Monitoring land degradation · Climate change · Semi-
arid region

Introduction

Semi-arid regions comprise nearly 15% of the total global area and host 15% of the global human

population (Millennium Ecosystem Assessment, 2005). Many uncertainties have arisen with respect to the potential effects of global change in these regions, especially regarding the impacts it could have on its ecosystems and what this entails for human welfare. Considering that these ecosystems provide food, energy, and grazing for livestock, among other ecosystem services, their sustainability is a major concern in the face of the desertification threats currently at play. Increasing evidence of temperature rise and a decrease in rainfall in semi-arid regions around the world (Christensen and Christensen, 2007; Dai, 2013) suggest that these semi-arid ecosystems will be negatively affected by increasing desertification processes (i.e., land degradation is characterized by a persistent reduction of biological and economic productivity (Millennium Ecosystem Assessment, 2005)). For example, northern Nigeria is located in a semi-arid region bordering the Sahara desert, averaging less than 600-mm annual rainfall. Although there are not many proper documents about the severity of the desertification in this zone, some reports suggest that 0.6 km per year is the rate of desertification. Visible signs of this phenomenon are not only the shift of vegetation ecosystems to expansive desert-like sand areas, also the drying up of water resources. Consequently, food insecurity increases due to less arable land and water for irrigation, then more anthropogenic effects unchain, like health problems and economic negative impacts (Olagunju, 2015).

This study focused on the semi-arid region of Chile, which is located south of the hyper-arid Atacama Desert, a region that is currently under the threat of desertification due to natural and anthropogenic drivers. Here, both a temperature rise and more frequent periods of prolonged droughts (i.e., El Niño Southern Oscillation) are expected (Meza, 2013). Vegetation productivity is a key metric for monitoring land degradation, because agriculture and livestock production are the primary economic activity and a key supporting ecosystem service. Within the study area, the natural vegetation composition varies as a result of the spatial heterogeneity associated with the mountainous topography and altitudinal gradient. Nevertheless, shrublands and seasonal grasslands are the main and secondary land cover types, respectively. These cover types have been largely degraded by overgrazing as a result of goat production and firewood extraction (Perez-Quezada et al., 2012), exposing soils to erosive processes, nutrient losses, and a reduction in their water retention capacity (Gutierrez

and Squeo, 2004). The overexploitation of scarce resources and less-productive vegetation due to changes in climate conditions are the key threats that have increased the vulnerability of the ecosystems in this semi-arid region.

Monitoring natural vegetation dynamics has become a very important strategy to detect the impacts of global change across ecosystems. Vegetation plays an important role for the hydrologic (evapotranspiration/interception) and biogeochemical cycles (photosynthesis/respiration), being an active regulator of the mass/energy exchange between the atmosphere and the terrestrial surface (Kariyeva et al., 2012). Therefore, if the relationship between climate and vegetation determines its distribution and growth dynamics, a shift in climate conditions can lead to changes in vegetation structure and functioning, affecting the ecosystem's water balance (Chen et al., 2014).

Moreover, human activity has intensively affected ecosystems through land-use change pressure, consequently leading to habitat destruction and biodiversity reduction, indicating the need to detect and predict changes in ecosystem functioning (Naeem et al., 1999).

The two main variables used in this work are productivity and phenology. Functional traits of ecosystems, associated mainly with the productivity variable, can be identified by the amount and seasonality of photosynthetic activity. This process is strongly associated with the aboveground net primary productivity of the vegetation cover (Tucker & Sellers 1986; Paruelo et al., 2000). Phenology, defined as the study of the timing of vegetation biological events regarding biotic and abiotic factors (Lieth, 1974), can serve as an indicator for recognizing, measuring, and monitoring the biological impacts of climate change on ecosystems (Bradley et al., 1999). Currently, there are a range of methods that could be used to measure productivity and phenology directly on the ground, but working at a regional scale would be very time consuming and expensive. Alternatively, the ecosystem functional traits can also be identified and monitored remotely, using vegetation indices derived from satellite imagery.

Satellite-borne sensors record the electromagnetic energy emitted or reflected by an object or surface in different bands of the electromagnetic spectrum, providing quantitative and spatially continuous surface data. The increased availability of this information in the recent decades has enabled its use in ecology to characterize landscape structure and more recently, to

determine the functional attributes of ecosystems at different spatial and temporal resolutions (Paruelo, 2008). Numerous studies have shown that normalized difference vegetation index (NDVI) data obtained from satellite images are directly related to ecosystem functionality, particularly the aboveground net primary productivity (Huete et al., 2002). The NDVI is based on optical measurements of the vegetation canopy and varies with leaf chlorophyll, leaf area, canopy cover, and structure. The combination of the spectral absorption region by the red chlorophyll, together with the reflectance signal generated in the near infrared (NIR) due to the structure of the mesophyll of leaves, permits a determination of the green and photosynthetic capacity of the vegetation through a normalized ratio:

$$\text{NDVI} = \frac{\rho_{\text{NIR}} - \rho_{\text{RED}}}{\rho_{\text{NIR}} + \rho_{\text{RED}}} \quad (1)$$

where ρ_{NIR} and ρ_{RED} are reflectance measurements in the NIR and red bands, respectively (Tucker, 1979).

The NDVI can be used to derive the land surface phenology, which provides temporal records of spatial patterns of vegetation growth dynamics within an area (Liang et al., 2011, Kariyeva et al., 2012). The land surface phenology derived from NDVI data has been used in global climate change studies, and has shown trends and responses in vegetation dynamics, such as an earlier start of the growing season (Van Leeuwen et al., 2010, 2013) and to represent vegetation interactions with climate-based factors (Nemani et al., 2003; Kariyeva et al., 2012). Additionally, long-term NDVI time series have been used to analyze and monitor the trends (Anyamba & Tucker, 2005; Fensholt et al., 2012) and responses of vegetation to environmental variables, such as climate (Fensholt and Rasmussen, 2011; Fensholt et al., 2012) and land use/cover type (Baldi et al., 2008; Van Leeuwen et al., 2013).

The first two objectives of this work were to analyze (i) the trends in land surface productivity and (ii) the phenological functional traits within the semi-arid region, specifically in the Limarí River Basin, using the newest generation NDVI time series data from moderate resolution imaging spectroradiometer MODIS. The analysis encompasses trend studies for different land cover classes, with the purpose of characterizing and examining land cover specific productivity and phenological trends during a 14-year time period of increased

drought severity. The third objective was to examine the relationship between the land surface productivity and climate variables (based on rainfall and temperature) in order to generate productivity projections in response to climate change scenarios.

Data and methods

Study area

The study was conducted in the Limarí River Basin, located in the semi-arid region of Chile between coordinates 30° 15' N, 71° 45' W and 31° 30' S, 70° 15' E, with a total area of 11,696 km² (Fig. 1). It is bounded by the extremely dry Atacama Desert to the north and by the Mediterranean Central Chile farther south. The main feature of the terrain is the Andes Range to the east, which reaches an altitude at 5500 m a.s.l. and gradually decreases to the west, coinciding with the Limarí River delta in the Pacific Ocean.

The study area has a semi-arid Mediterranean climate regimen with spatial intra- and inter-annual variations. The cumulate annual precipitation ranges from 100 mm in the coastal area to 300 mm in the Andean region, averaging 125.7 mm annually (Verbist et al., 2010). The inter-annual variability of precipitation is linked to climatic events that occur irregularly at intervals between 2 and 7 years, with positive rainfall anomalies during El Niño events and below normal rainfall anomalies during the La Niña cycle (Verbist et al., 2010).

The mean annual temperature is 16.6 °C, with a minimum and maximum of 9.4 and 23.8 °C, respectively. Minimums occur during the winter season, coinciding with precipitation and snow events over 1000 m a.s.l., allowing snow accumulation in winter and snowmelt in the following seasons, often resulting in high stream flows during the late spring and summer months (Vicuña et al., 2011).

The national cadaster of land use and vegetation (CONAF, 2004) states that the main cover is natural vegetation (77%), followed by barren soil (18.3%) and agriculture (3.3%). Three main natural vegetation types dominate the landscape: (1) coastal shrublands and grasslands, characterized by fog-dependent species, mainly bushes and succulents, (2) inland shrublands and grasslands, present in the interior of the valley, occupying plains and hills and characterized by more xerophytic species, and (3) high Andean steppe, over

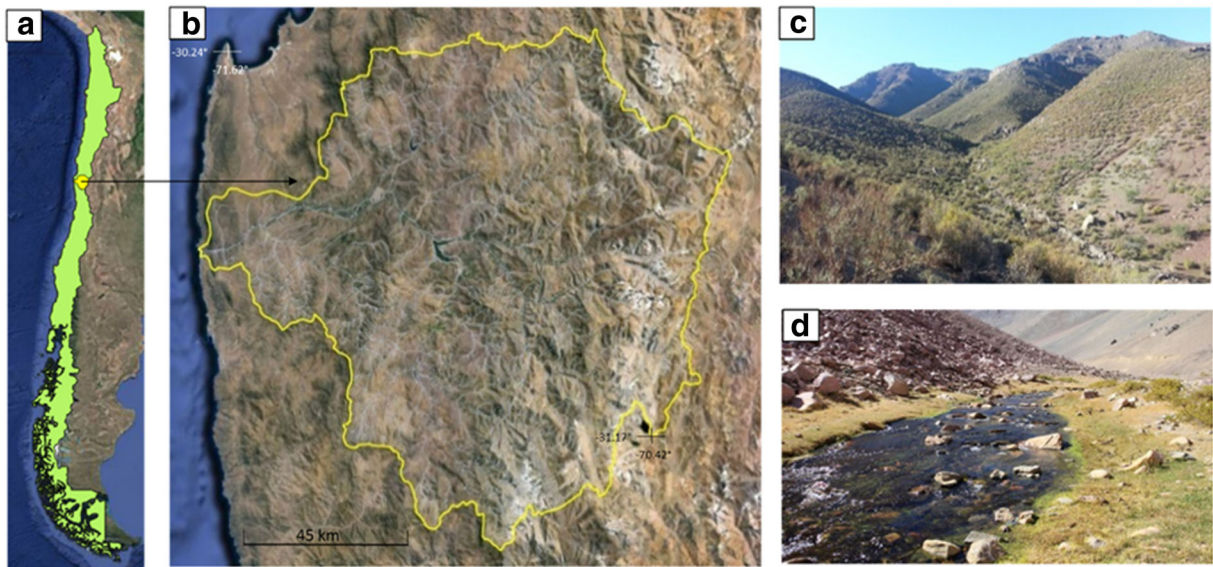


Fig. 1 Study area. **a** Chile—outlined in *green*. **b** Limari River Basin delimitation outlined with a *yellow line*. **c** A general view of the savanna-like landscape in the mid-basin. **d** An example of the high Andean steppe landscape over 2000 m elevation

2000 m a.s.l. including sparse bushes and peatlands (CONAF, 2004). Agricultural land cover is concentrated alongside rivers and streams in the valley and mainly consists of perennial fruit cultivars (annual crops and vineyards) (Parga et al., 2006).

MODIS vegetation productivity and phenology

NDVI time series data at 16-day composite intervals and 250-m spatial resolution (MOD13Q1 product from www.daac.ornl.gov/MODIS) were used to calculate the phenological metrics analyzed in this study. Three metrics were generated with this information: spring productivity (SP_{NDVI}), start of season (SOS), and seasonal amplitude (AMP). SP_{NDVI} represents the accumulated spring primary productivity and was generated by combining the NDVI data values from October to December for each year. SOS is a timing metric that represents the Julian day when vegetation productivity starts its annual activity. SOS corresponds to the time (day of year) at which the NDVI of a pixel increases by 10% with respect to the difference between the baseline NDVI and the maximum NDVI for that season (Jönsson & Eklundh, 2004). Seasonal amplitude is a vegetation greenness metric represented by the difference between the peak NDVI value and the average of the NDVI values at the start and end of the growing season. Both, yearly SOS and AMP, are land

surface phenological metrics obtained by processing the NDVI time series data using the TIMESAT software (Jönsson & Eklundh, 2004; www.nateko.lu.se/timesat). These three annual metrics were generated for the study site from 2000 to 2013, resulting in a total of 42 images (14 per metric) that was subsequently used in the inter-annual trend and climate scenario analyses.

Satellite temperature and rainfall

Temperature data were based on the MODIS 8-day LST/E product (MOD11A2) from 2000 to 2013. Land surface temperature images have a 1-km pixel resolution and temperature data are expressed in degrees Kelvin. The winter thermal sums (T) from July 11th through September 29th were used because pre-season temperature is a critical environmental factor that affects the inter-annual variability of spring phenology (Wang et al., 2015). Degrees Kelvin were converted to degrees Celsius and negative values to 0 °C, under the assumption that this temperature was the threshold for low vegetation activity and negative temperatures would not make a significant difference to the very low NDVI values obtained on those dates. Finally, a yearly winter thermal sum value was obtained by summing all of the T images from 11/6 through 29/9 (corresponding to composites 24 to 34, respectively).

Due to insufficient rain gauge datasets, the Tropical Rainfall Measuring Mission (TRMM) satellite products were used as a proxy for the spatial distribution of rainfall at the study site. The TRMM was designed to examine the precipitation structure, rate, and distribution for latitude ranges $\pm 50^\circ$ (Kummerow and Barnes, 1998). Castro et al. (2015) analyzed TRMM-derived precipitation in the central Andes range, with a Mediterranean climate, and established a good performance for medium magnitude rainfall events; however, relief and snow negatively affected the estimates. Precipitation data consisted of the monthly multi-satellite precipitation analysis (TMPA 3B43 version 7) product on a $0.25^\circ \times 0.25^\circ$ latitude-longitude grid (NASA Earth Observing System Data and Information System, EOSDIS, 2013). Monthly data was summed for each year to generate annual rainfall (PP) from 2000 to 2013. To avoid the spatial inconsistencies of rainfall data, the average rainfall of all TRMM pixels was used, removing pixels that were located above the mean elevation (1500 m a.s.l.).

Productivity and phenology trends

The NDVI time series-based metrics provided the basis for examining trends in ecosystem productivity and phenological dynamics at different elevation levels and for different types of land cover. Regressions of the three metrics were developed using time functions in a linear model and computed on a pixel by pixel basis:

$$y_i = a_i + \beta_i * x_i + \varepsilon_i \tag{2}$$

where y_i is the functional metric based on NDVI (SP_{NDVI} , SOS, or AMP) for a specific pixel i , and a_i , β_i , and ε_i are the intercept, slope coefficient, and residual of the linear regression for the same pixel (i), respectively. Significant trends in the annual metrics were determined based on the slope coefficient (β) of the simple linear regression model described above (Van Leeuwen et al., 2013), considering a p value ≤ 0.1 .

Analysis of the relationship between productivity and climate data

To examine the relationship between climatic variables and ecosystem productivity, a multiple linear regression

was applied, using PP and T , as explanatory variables, and SP_{NDVI} as the response variable:

$$SP_{NDVI} = a_i + b_i \times PP_i + c_i \times T_i + \varepsilon_i \tag{3}$$

where a_i is the regression intercept for pixel i , b_i and c_i are the slope coefficients for PP and T for pixel i , respectively, and ε_i is the residual at the pixel level.

For each pixel, the slope regression coefficients of both explanatory variables were used to examine the independent effects of the climatic variables on spring productivity. A 90% confidence level was used in the analyses because semi-arid systems are spatially and seasonally variable, essentially implying a heterogeneous data structure. Moreover, images with coarser spatial resolutions were resampled to 250×250 m, allowing the maximum amount of heterogeneity in the response variables to drive the analyses and results.

Productivity projections and climate change scenarios

To achieve the third objective of this study, productivity projections were obtained by substituting projected climate data in the multiple linear regression model (Eq. 3) using temperature and precipitation data from ground stations, instead of the LST (T) and TRMM (PP) sensors. Projected climate data were obtained by a three-step weather generator downscaling method. The first step was the extraction of the probabilistic trends in temperature and precipitation from several global climate models. The second step generated yearly temperature and precipitation data using the extracted trends for the different station gauges of the basin, and the third step consisted of a K-nearest neighbor (K-NN) disaggregation method applied to monthly precipitation and temperature data. This method considers the natural variability, making it necessary to use several realization series. In our study, the yearly average of 100 series was used.

Two stations at different altitudes were selected for climatic projection: La Paloma Embalse (30.7° S 71.03° W, 320 m a.s.l.) and Las Ramadas (31° S 70.6° W, 1380 m a.s.l.). For each station, representative pixels with similar rainfall data were selected within a 3-km radius. Representative concentration pathway (RCP) climate change scenarios were selected to obtain PP and T projections from 1980 to 2100. RCP 8.5 represents a high-emission scenario, in which radiative forcing reaches over 8.5 W/m^2 by 2100 and continues to rise, while RCP 2.6 represents a scenario where radiative forcing peaks at

approximately 3 W/m² before 2100 and then declines (van Vuuren et al., 2011). These data were used within the multiple linear regression models to obtain the mean projected productivity of the 1981–2020, 2021–2060, and 2061–2100 periods. Finally, the productivity changes (expressed as a percentage of the baseline values) in natural vegetation pixels surrounding the stations were evaluated using the 1981–2020 temperature and precipitation projections as a basis for comparison.

Results

Vegetation spring productivity and phenological trends

There was a steady decline in the value of SP_{NDVI} within the Limarí River Basin from 2000 to 2013 (Fig. 2). Of the land area, 61.4% displayed a significant negative trend ($p < 0.1$), affecting 974,000 ha that were mainly located below 2000 m a.s.l. On the other hand, 10.3% of the surface displayed positive SP_{NDVI} trends ($p < 0.1$), with 90% of these areas located above 2000 m. The remaining 28.2% of the surface had no significant SP_{NDVI} trend. The average annual change in productivity was -2.45% with respect to the mean SP_{NDVI} (Table 1).

The majority of the surface area (78.4%) did not show a significant SOS trend, while 19.1% of the surface area (mainly located above 2000 m a.s.l.) displayed a negative trend implying an earlier SOS (Table 1). This compartment showed a clear phenological difference between low and mid-elevation vegetation cover and high-elevation vegetation cover. In contrast, the remaining 2.5% of the surface area displayed a positive SOS trend (later SOS) and was concentrated mainly in the lower part of the basin. The SOS average for higher elevation vegetation cover was at Julian day 230 (August) and had a negative trend of -5 days per year. In the lower part of the basin, the SOS was at day 180 (June), displaying positive trends and with SOS beginning 6 days later per year.

Similar to the SOS phenological metric, the amplitude did not show a significant trend in most (almost 80%) of the surface area, but a statistically significant negative trend was observed in areas with a high elevation (Fig. 2), mostly at a mean altitude of 2800 m. The mean amplitude was 0.2 NDVI units, while the pixels with a negative trend averaged -0.007 NDVI units per year.

The SP_{NDVI} relationship with precipitation and temperature

The results obtained from the multiple linear regression between PP, T , and SP_{NDVI} as a dependent variable indicated that 68.7% of the whole study area exhibited significant vegetation responses to precipitation (Table 2). These significant values, as seen in Fig. 3a, were mainly positive slope pixels, denoting a direct relationship between PP and SP_{NDVI} below 2000 m. Conversely, in the upper basin, a significant number of pixels had negative slope values, implying an indirect relationship between rainfall and spring productivity. In contrast to PP, there were significant values related to temperature across 38.3% of the whole area (Fig. 3b), with positive slope pixels in highlands and negative slope pixels in lowlands (Table 2).

Finally, Fig. 4 shows how the SP_{NDVI} trends are distributed spatially in the basin and how these trends behave in relation to precipitation and temperature. Vegetation along river streams (riparian and agriculture cover classes) did not show significant trends or significant values for PP and T . Positive SP_{NDVI} trends were observed in the upper basin, with significant PP and T relationships for some pixels. Negative trends were mainly related to PP in the mid-basin and to T in the low basin.

The highest positive PP slopes were indicative of the strong influence of precipitation on semi-arid vegetation. According to the regression model, each additional mm/year would increase the SP_{NDVI} by 0.035 units (0.19% of the mean SP_{NDVI}, Table 2.)

SP_{NDVI} projections for the RCP 2.6 and 8.5 climate change scenarios

After examining land pixels within a 3-km radius around the weather stations, 471 pixels were selected for La Paloma station and 252 for Las Ramadas, using the significant multiple linear regression results as a selection criteria. The majority of these had significant relationships with the PP variable (Fig. 5). La Paloma station (located at 320 m a.s.l.) had a greater SP_{NDVI} decline compared to Las Ramadas (1380 m a.s.l.) station using the projected future climate data (Fig. 6). There was an 11.72% productivity decrease in the 2060–2100 period compared to the baseline period (1981–2020) when using RCP 8.5 scenario for La Paloma, while for Las Ramadas, this decrease was 3.26% for the same

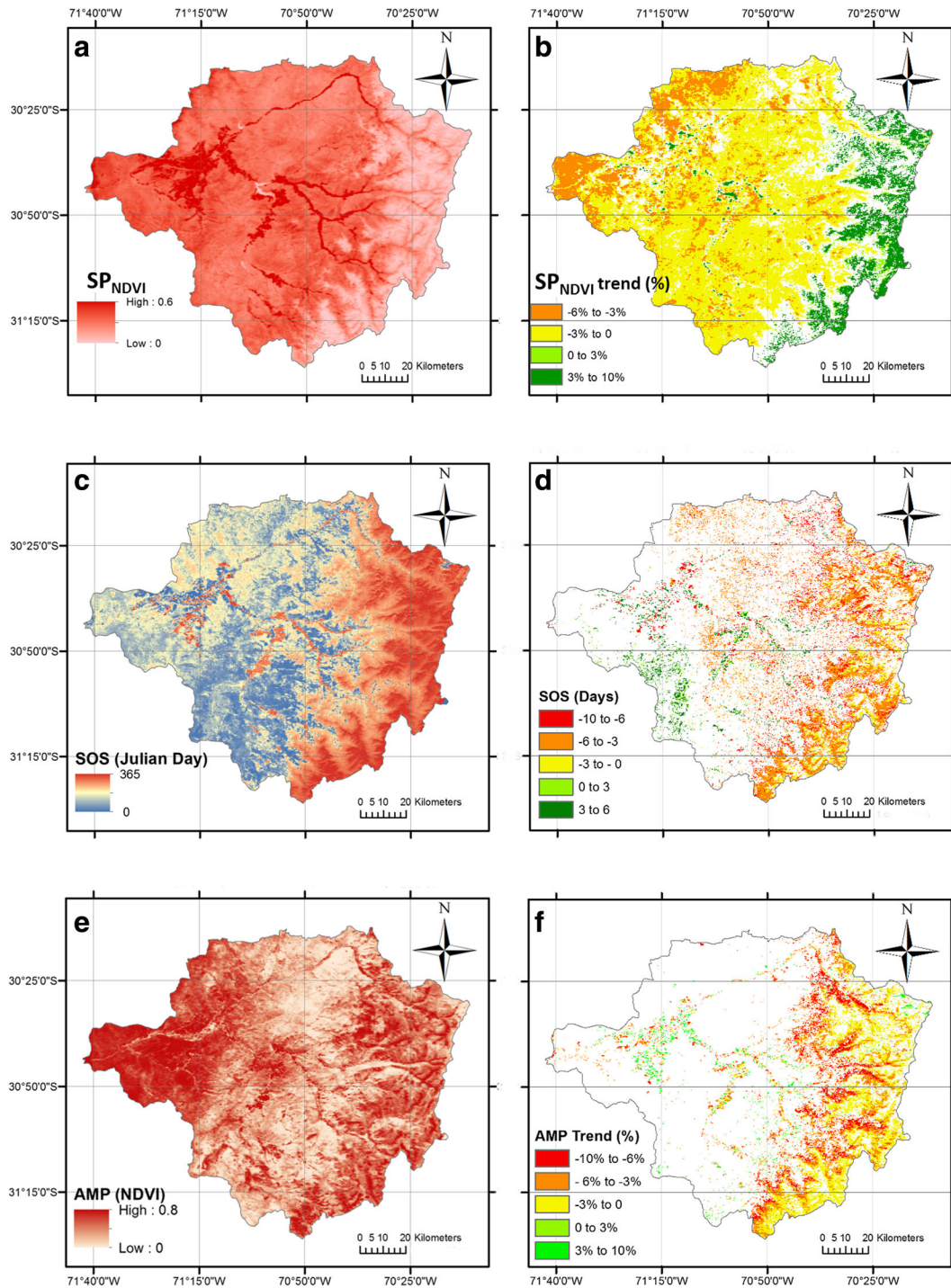


Fig. 2 Average (2000–2013) values of productivity (SP_{NDVI} average spring NDVI values) and phenological variables (SOS start of season—Julian day, AMP - NDVI seasonal amplitude—represented by the difference between baseline and maximum NDVI value) are

shown in (a), (c), and (e), respectively (left hand side). Annual change rates are represented by the linear regression slope values for SP_{NDVI} (b), SOS (d), and AMP (f) (right hand side). White pixels represent non-significant trend values

Table 1 Summary of significant ($p \leq 0.1$) vegetation productivity (SP_{NDVI}) and land surface phenological trends and their associated spatial extent and annual rate of change from 2000 to 2013

Productivity and phenology metrics	Trend	Total surface (thousand ha)	Total surface (%)	Mean slope value	Metric mean (2000–2013)	% rate of change (slope*100/mean)
SP_{NDVI}	Negative	974	61.4	-0.005*	0.22*	-2.45
	Positive	163	10.3	0.003*	0.08*	5.81
AMP	Negative	323.5	20.4	-0.007	0.20	-3.89
	Positive	20.5	1.3	0.009	0.21	4.22
SOS	Negative	303.4	19.1	-5	230.4	-1.3**
	Positive	39	2.5	5.79	179.9	1.58**

AMP amplitude, SOS start of the growing season

* SP_{NDVI} : values are daily average NDVI units

**SOS % rate of change is over 365 days

scenario (Table 3). As expected, the RCP 8.5 scenario resulted in higher vegetation productivity decreases than the RCP 2.6 scenario. Nevertheless, La Paloma always displayed a greater decline regardless of the climate scenario.

As seen in Table 3, the PP- and T -related pixels indicated a large decrease in productivity for La Paloma (-19% in RCP 8.5 and -7.86% in RCP 2.6), while in Las Ramadas, the projections indicated an increase in productivity (3.62% in RCP 8.5).

Discussion

Inter-annual trends of vegetation productivity and phenological functional traits were analyzed using MODIS NDVI 2000–2013 time series data. The results showed a general decrease in vegetation spring productivity over this period for practically all of the study sites below 2000 m a.s.l., which were mainly composed of shrublands with different densities. Moreover, the analysis of climatic variables in the relationship with

productivity trends suggests that precipitation explained this reduction in productivity for most of the lower basin. Temperature is also relevant but mostly in lower areas below 500 m a.s.l. Finally, future productivity projections suggest that lower altitude natural vegetation will undergo a more severe decline than vegetation in the higher basin.

At this regional scale, a wide variety of natural vegetation communities, with different dynamics, could be identified along the elevation gradient. The 14-year productivity and phenology trend analysis showed contrasting results among the elevation cline. In the higher altitudes of the basin, spring productivity displayed positive trends with temperature. Nevertheless, NDVI amplitude trends in these areas were negative, suggesting that higher winter temperatures reduced the difference between baseline and peak NDVI values. Furthermore, areas with negative SOS trends (earlier start of growing season) were also observed in these areas. Similar behavior has been observed by Van Leeuwen et al. (2013) using a 1982–2011 advanced very high resolution radiometer NDVI time series data for South

Table 2 Overview of the multiple linear regression results, in which productivity was a function of precipitation and temperature. The results show significant slope values for the whole extent and the percentage rate of change of NDVI relative to the mean NDVI

Environmental variables	Slope	Surface (thousand ha)	Percentage of total extent (%)	Mean slope regression coefficient	Percentage rate of change with respect to mean NDVI (%)
Precipitation	Negative	168.9	10.64	-0.015	-0.084
	Positive	921.5	58.07	0.035	0.195
Temperature	Negative	297.5	18.74	-0.019	-0.106
	Positive	310	19.53	0.012	0.065

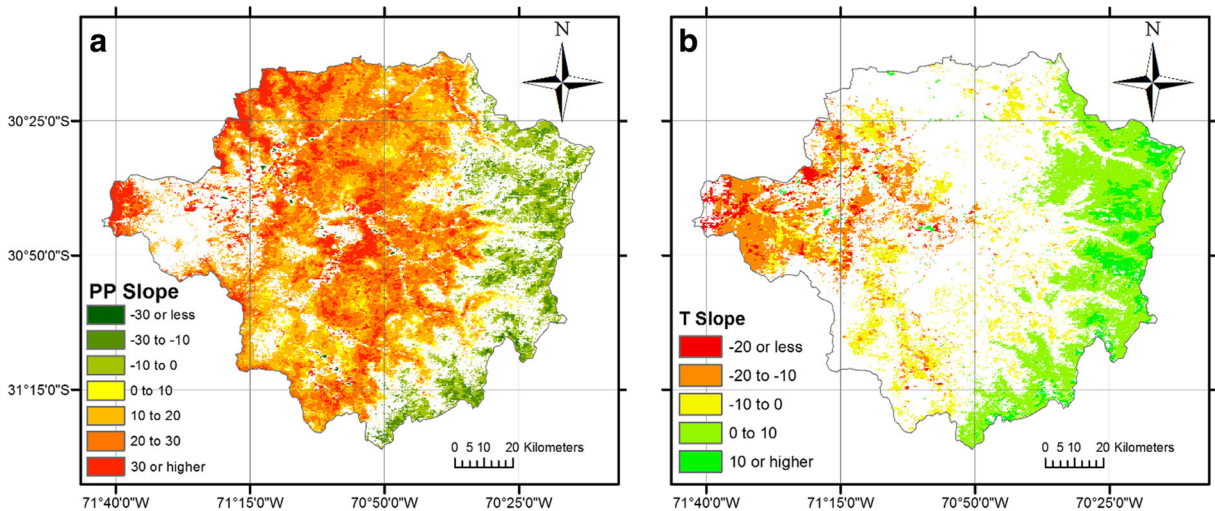


Fig. 3 a The productivity-precipitation relationship expressed by the significant NDVI/PP slope values obtained from the multiple linear regressions between SP_{NDVI} as a function of PP. b The productivity-temperature relationship expressed by the significant

slope values obtained from the multiple linear regression between SP_{NDVI} as a function of T . *White pixels* represent non-significant slope values. Legend values are $\times 10,000$ their original values in NDVI units per 1 mm in (a) and per 1 °C in (b)

America. The results indicate that highland vegetation in semi-arid regions had undergone a phenological shift, governed by an earlier start of the season, which could explain the greater spring productivity. Higher winter temperatures generate an earlier snowmelt, allowing the sparse vegetation, and peatlands to begin photosynthetic activity sooner than expected. Moreover, this vegetation displayed a negative amplitude trend, which was

probably related to the higher NDVI value at the start of their season and/or a lower NDVI value for the seasonal peak. In conjunction, Jeganathan et al. (2014) found a decreasing trend in the seasonal amplitude in high latitudes from 1997 until the present day. The relationship between precipitation and productivity in the upper basin showed that wetter years would result in less productivity. These results are consistent with

Fig. 4 Spatial relation between SP_{NDVI} trends from 2000 to 2013, and the response of NDVI to precipitation and temperature, as represented by significant NDVI/PP and NDVI/T slopes. *NS* not significant

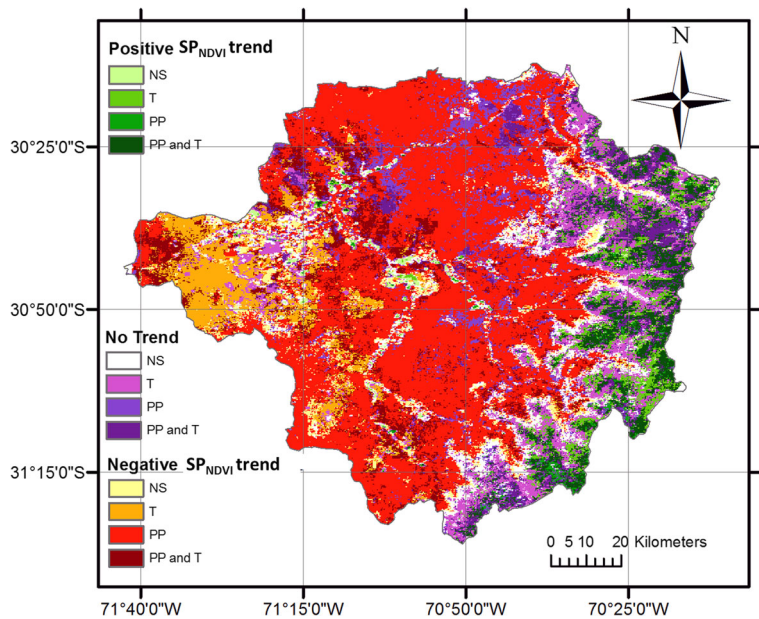
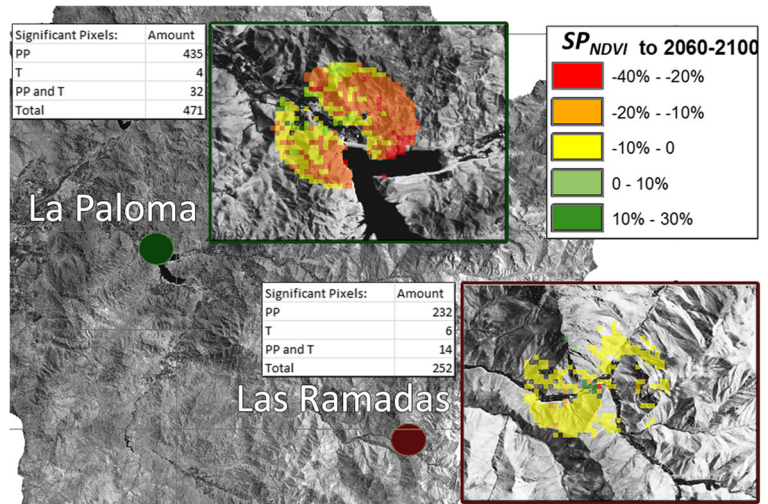


Fig. 5 La Paloma and Las Ramadas stations in Limari River Basin. Circles represent the 3-km radius area used to select pixels. Pixels are presented in colors, representing the productivity change in the 2060–2100 period using the 1981–2020 period as a basis for comparison



Squeo et al. (2006) who found that the spring productivity of highland vegetation (over 2500 m a.s.l.) decreased in rainy years, while it increased in drier years, probably due to the colder temperatures in rainy years. Below 2000 m a.s.l., there were strong productivity/climate relationships, with no significant phenological trends.

The high number of significant pixels that were dependent on precipitation confirmed the strong effects it has on the variability of inter-annual productivity. Shrublands, which were the main ecosystems in the semi-arid basin below 2000 m a.s.l., had clear negative productivity trends, with a predominantly positive relationship with precipitation. Many authors have consistently found NDVI anomalies related to precipitation irregularities in semi-arid and arid regions (Nezlin et al., 2005, Fensholt et al., 2012), emphasizing that rainfall is a limiting factor for vegetation growth. Some other studies have included temperature in their analysis and have found positive correlations with the NDVI in inter-seasonal analysis (Propastin et al., 2006, Eckert et al., 2015). The productivity decline is higher when the relation with precipitation and/or temperature is stronger, with precipitation being a greater contributor due to the vegetation-water-dependence. In the lower basin (below 500 m a.s.l.), where coastal fog influences vegetation (Gutiérrez and Squeo, 2004) with high daily humidity, temperature dependent pixels displayed a negative relation between T and productivity. The shrubland/grassland vegetation of these lowland areas might be affected by higher evaporation rates,

decreasing the chances of moisture transpiration. Kariyeva et al. (2012) related decreasing productivity values with higher temperatures using remotely sensed data for Central Asia. Furthermore, Barron-Gafford et al. (2012) reported that increasing temperatures could negatively impact plant growth and increase water stress, principally in semi-arid grassland ecosystems.

The future productivity projections in this study were assumed to be linearly dependent on ground-measured PP and T values, meaning that the productivity projections were dependent on the magnitude of the slopes and projected climate values. The projected productivity values for lower elevation locations displayed higher rates of decline than higher elevation locations regardless of the percentage decrease in precipitation, which was the same for both stations. This depended mainly on the precipitation slope values, which were four times higher at La Paloma station (low altitude) than at Las Ramadas station (high altitude). Moreover, lower elevation vegetation had more significant pixels related to temperature (T), with negative slope values that intensified the productivity decline due to the higher projected temperatures. Whereas lower elevation areas had less rainfall than higher areas, the results indicated that the vegetation established in dryer areas was more dependent on the rainfall regime. Therefore, its productivity would be more prone to a shift if these regimes changed. As shown in Table 3, a 20% rainfall decrease in the La Paloma area would

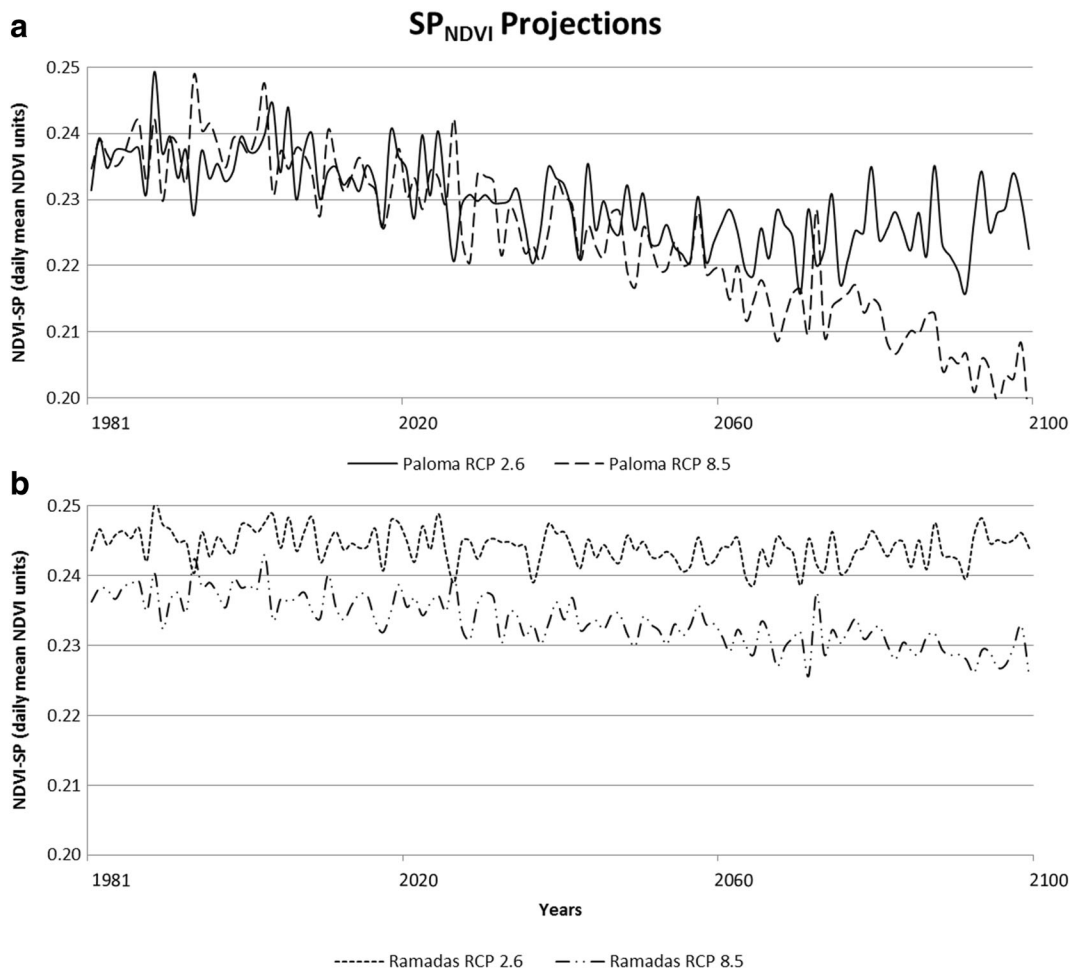


Fig. 6 Projected productivity (SP_{NDVI}) values from 1981 to 2100 for two RCP scenarios. **a** La Paloma station. **b** Ramada station

imply a decline in productivity of about 12% when projected to the end of this century.

Certain environmental processes and ecosystem functions, such as water and energy fluxes, erosion

Table 3 Overall productivity projections for vegetation near La Paloma and Las Ramadas stations for the RCP 2.6 and 8.5 scenarios. The percentage change is with respect to the mean projected productivity for the period of 1981–2020

Period	All pixels		PP-related pixels		T-related pixels		PP- and T-related pixels	
	2021–2060 (%)	2061–2100 (%)	2021–2060 (%)	2061–2100 (%)	2021–2060 (%)	2061–2100 (%)	2021–2060 (%)	2061–2100 (%)
La Paloma (RCP 2.6)	-3.26	-4.57	-3.04	-4.24	-9.63	-14.62	-5.36	-7.86
La Paloma (RCP 8.5)	-4.72	-11.72	-4.19	-10.08	-12.89	-35.7	-7.26	-19
Las Ramadas (RCP 2.6)	-0.74	-0.85	-0.80	-0.94	-0.71	-0.8	0.72	1.51
Las Ramadas (RCP 8.5)	-1.50	-3.26	-1.62	-3.57	-2.53	-7.20	0.09	3.62

rates, fodder production, and agricultural yields, are linked to vegetation productivity (Gessner et al., 2013). Although these relations were outside the scope of our study, high declining productivity areas are probably the most vulnerable and prone to desertification. This process is self-accelerating, with land degradation resulting in the destruction of the land's productive potential (Nezlin et al., 2005). Further interdisciplinary studies are needed to better understand the physiological mechanisms by which vegetation responds to precipitation and temperature changes.

Anthropogenic pressures, such as land-use change, livestock grazing, and wood extraction, were not included in the analysis as drivers of change and were beyond the scope of this study. The exposure and proximity of vegetation to human settlements could therefore have influenced the NDVI signal during the study period, expanding the actual reduction. Although it was not measured in this study, Blanco et al. (2008) analyzed the grazing effects on annual net primary productivity using the NDVI for semi-arid rangeland in Argentina and observed a greater grazing impact in drier years. Both studies could be used to measure the spatial vulnerability, including natural and anthropogenic factors. The short analysis period (14 years) was another limitation, because trends obtained from linear regressions could be more strongly influenced by the severe drought that this region has experienced in the recent years. The analysis of longer time periods could include the effects of the ENSO phenomenon. Nevertheless, studying the particular effects of climatic anomalies on vegetation activity could provide complementary information regarding the trends in the vegetation response to climate variables (Gessner et al., 2013). Spatially distributed moderate resolution precipitation data would improve the significance of our results and might also help further analyze temporal lags and accumulation periods. Finally, the results obtained in this work can nourish other interesting areas of studies such as effects of land degradation (in terms of the potential primary productivity), in the human well-being considering bioclimatic comfort and health (Cetin, 2015), availability of provisioning and ecosystem services support, land-use planning and policies, monitoring of species and functional biodiversity, and among others. This new knowledge can be used by specialist in the development of new plans and policies oriented to adapt the society to the new scenarios of climate change that are transforming the biosphere.

Conclusions

Semi-arid ecosystems are impacted by reduced water availability and anthropic pressure. This is a key concern for the increasing social and environmental vulnerability of these areas. Ecosystems are threatened not only by direct human-induced impacts but also by indirect global climate change. Changing climate patterns makes ecosystem resilience an essential quality to ensure their adaptive capacity and the sustainability of their ecological processes. Managing our landscapes under changing earth system conditions makes it even more necessary to analyze and monitor vegetation conditions and responses to climate variables. Climate and remotely sensed time series data serve as a useful tool.

The aim of this study was to provide a better understanding of the spatial distribution of changes in a semi-arid ecosystem in response to a changing climate at the regional scale, including an elevation gradient. To achieve this, and to ensure that the method could be reproduced in other regions, remote sensing with a high temporal resolution was used. Easily accessible and consistent MODIS global data provided for replicability and will allow for ongoing analysis to determine trends in vegetation-climate dynamics.

Phenology, productivity, and climate maps have helped to identify the range of land cover and elevation zones in which changes are occurring, and where they could be attributed to precipitation and/or temperature shifts. The interactions between land surface productivity, phenology, and climate variables were complex and seemed to stratify within a continuum of land cover types and elevation gradients. Future productivity projections can be used to monitor and understand the sensitivity of vegetation to climate change impacts. Moreover, this information allows us to identify ecosystems that are vulnerable to climate change, so encouraging future research, monitoring, and management programs to examine the adaptability and resilience of changing ecosystems. Land managers and decision-makers, with land exposed to climate change, can consider this information for planning land-use changes and adaptive management strategies.

Acknowledgements This research was funded by a FONDEF grant (number D10I1051). Support was also provided by a grant (CRN3056) from the Inter American Institute for Global Change Research.

The MOD13Q1 and MOD11A2 data products were provided courtesy of the online Data Pool at the NASA Land Processes Distributed Active Archive Center, USGS/Earth Resources Observation, and Science Center, Sioux Falls, South Dakota (https://lpdaac.usgs.gov/data_access).

References

Anyamba, A., & Tucker, C. J. (2005). Analysis of Sahelian vegetation dynamics using NOAA-AVHRR NDVI data from 1981–2003. *Journal of Arid Environments*, 63, 596–614.

Baldi, G., Nasetto, M. D., Aragón, R., Aversa, F., Paruelo, J. M., & Jobbágy, E. G. (2008). Long-term satellite NDVI data sets: evaluating their ability to detect ecosystem functional changes in South America. *Sensors*, 8, 5397–5425.

Blanco, L. J., Aguilera, M. O., Paruelo, J. M., & Biurrun, F. N. (2008). Grazing effect on NDVI across an aridity gradient in Argentina. *Journal of Arid Environments*, 72(5), 764–776.

Bradley, N. L., Leopold, A. C., Ross, J., & Huffaker, W. (1999). Phenological changes reflect climate change in Wisconsin. *Proceedings of the National Academy of Sciences of the United States of America*, 96, 9701–9704.

Barron-Gafford, G. A., Scott, R. L., Jenerette, G. D., Hamerlynck, E. P., & Huxman, T. E. (2012). Temperature and precipitation controls over leaf-and ecosystem-level CO₂ flux along a woody plant encroachment gradient. *Global Change Biology*, 18(4), 1389–1400.

Castro, L. M., Miranda, M., & Fernández, B. (2015). Evaluation of TRMM multi-satellite precipitation analysis (TMPA) in a mountainous region of the central Andes range with a Mediterranean climate. *Hydrology Research*, 46(1), 89–105.

Cetin, M. (2015). Determining the bioclimatic comfort in Kastamonu City. *Environmental Monitoring and Assessment*, 187(10). doi:10.1007/s10661-015-4861-3.

Chen, C., Eamus, D., Cleverly, J., Boulain, N., Cook, P., Zhang, L., Cheng, L., & Yu, Q. (2014). Modelling vegetation water-use and groundwater recharge as affected by climate variability in an arid-zone Acacia savanna woodland. *Journal of Hydrology*, 519, 1084–1096.

Christensen, J. H., & Christensen, O. B. (2007). A summary of the PRUDENCE model projections of changes in European climate by the end of this century. *Climatic Change*, 81(1), 7–30.

Corporación Nacional Forestal (CONAF), 2004. Catastro y Evaluación de Usos del Suelo y Vegetación, Cuarta Región. Coquimbo. Chile. 32 pp.

Dai, A. (2013). Increasing drought under global warming in observations and models. *Nature Climate Change*, 3, 52–58.

Eckert, S., Hüslér, F., Liniger, H., & Hodel, E. (2015). Trend analysis of MODIS NDVI time series for detecting land degradation and regeneration in Mongolia. *Journal of Arid Environments*, 113, 16–28.

Fensholt, R., Langanke, T., Rasmussen, K., Reenberg, A., Prince, S. D., Tucker, C., et al. (2012). Greenness in semi-arid areas across the globe 1981–2007—an earth observing satellite based analysis of trends and drivers. *Remote Sensing of Environment*, 121, 144–158.

Fensholt, R., & Rasmussen, K. (2011). Analysis of trends in the Sahelian ‘rain-use efficiency’ using GIMMS NDVI, RFE and GPCP rainfall data. *Remote Sensing of Environment*, 115(2), 438–451.

Gessner, U., Naeimi, V., Klein, I., Kuenzer, C., Klein, D., & Dech, S. (2013). The relationship between precipitation anomalies and satellite-derived vegetation activity in Central Asia. *Global and Planetary Change*, 110, 74–87.

Gutiérrez, J. R., & Squeo, F. A. (2004). Importancia de los arbustos en los ecosistemas semiáridos de Chile. *Ecosistemas: Revista Científica y Técnica de Ecología y Medio Ambiente*, 13, 36–45.

Huete, A., Didan, K., Miura, T., Rodriguez, E., Gao, X., & Ferreira, L. (2002). Overview of the radiometric and biophysical performance of the MODIS vegetation indices. *Remote Sensing of Environment*, 83, 195–213.

Jeganathan, C., Dash, J., & Atkinson, P. M. (2014). Remotely sensed trends in the phenology of northern high latitude terrestrial vegetation, controlling for land cover change and vegetation type. *Remote Sensing of Environment*, 143, 154–170.

Jönsson, P., & Eklundh, L. (2004). TIMESAT—a program for analyzing time-series of satellite sensor data. *Computers & Geosciences*, 30, 833–845.

Kariyeva, J., van Leeuwen, W. J. D., & Woodhouse, C. A. (2012). Impacts of climate gradients on the vegetation phenology of major land use types in Central Asia (1981–2008). *Frontiers of Earth Science*, 6, 206–225.

Kummerow, C., & Barnes, W. (1998). The tropical rainfall measuring mission (TRMM) sensor package. *Journal of Atmospheric and Oceanic Technology*, 15, 809–819.

Liang, L., Schwartz, M. D., & Fei, S. (2011). Validating satellite phenology through intensive ground observation and landscape scaling in a mixed seasonal forest. *Remote Sensing of Environment*, 115, 143–157.

Lieth, H. (1974). *Phenology and seasonality modeling*. Berlin, Heidelberg: Springer Berlin Heidelberg.

Meza, F. J. (2013). Recent trends and ENSO influence on droughts in northern Chile: an application of the standardized precipitation evapotranspiration index. *Weather and Climate Extremes*, 1, 51–58.

Millennium Ecosystem Assessment. 2005. Ecosystem and human wellbeing. Desertification synthesis. Washington DC: World resource Institute <http://www.maweb.org/documents/document.355.aspx.pdf>

Naeem, S., Chapin III, F.S., Constanza, R., Ehrlich, P.R., Golley, F.B., Hooper, D.U., Lawton, J.H., O’Neill, R. V., Mooney, H. A., Sala, O. E., Symstad, A. J., Tilman, D., 1999. Biodiversity and ecosystem functioning: maintaining natural life support processes. <http://www.cricyt.edu.ar/institutos/iadiza/ojeda/BiodiFuncio.htm>, Nov 14, 2014.

NASA Earth Observing System Data and Information System (EOSDIS), 2013. Multi-satellite precipitation analysis (TMPA 3B43 version 7, product on a 0.25° × 0.25° latitude-longitude grid (<http://disc.sci.gsfc.nasa.gov/SSW>).

Nemani, R. R., Keeling, C. D., Hashimoto, H., Jolly, W. M., Piper, S. C., Tucker, C. J., Myneni, R. B., & Running, S. W. (2003). Climate-driven increases in global terrestrial net primary production from 1982 to 1999. *Science (New York, N.Y.)*, 300, 1560–1563.

- Nezlin, N. P., Kostianoy, A. G., & Li, B.-L. (2005). Inter-annual variability and interaction of remote-sensed vegetation index and atmospheric precipitation in the Aral Sea region. *Journal of Arid Environments*, 62(4), 677–700.
- Olagunju, T. E. (2015). Drought, desertification and the Nigerian environment: a review. *Journal of Ecology and The Natural Environment*, 7(7), 196–209.
- Parga, F., León, A., Vargas, X., Fuster, Y., 2006. El índice de pobreza hídrica aplicado a la cuenca del río Limarí en Chile semiárido. Eval. Usos del Agua en Tierras Secas de Iberoamérica, 93–109.
- Paruelo, J. M. (2008). La caracterización funcional de ecosistemas mediante sensores remotos. *Revista Ecosistemas*, 17(3), 4–22.
- Paruelo, J. M., Oesterheld, M., Bella, D., Carlos, M., Arzadum, M., Lafontaine, J., Cahuepé, M., & Rebella, C. M. (2000). Estimation of primary production of subhumid rangelands from remote sensing data. *Applied Vegetation Science*, 3, 189–195.
- Perez-Quezada, J. F., Bown, H. E., Fuentes, J. P., Alfaro, F. A., & Franck, N. (2012). Effects of afforestation on soil respiration in an arid shrubland in Chile. *Journal of Arid Environments*, 83, 45–53.
- Propastin, P.P., Kappas, M., Muratova, N.R., 2006. Temporal responses of vegetation to climatic factors in Kazakhstan and Middle Asia, shaping the change. XXIII FIG Congress, Munich, Germany, pp. 16.
- Squeo, F.A., Ibacache, E., Warner B., Espinoza D., Aravena R., Gutiérrez J.R., 2006. Productividad y diversidad florística de la Vega Los Tambos, Cordillera de Doña Ana: variabilidad interanual, herbivoría y nivel freático. Geoecología de los Andes Desérticos: La Alta Montaña del Valle del Elqui, Ediciones Universidad de La Serena, La Serena, Chile, pp. 333–362.
- Tucker, C. J. (1979). Red and photographic infrared linear combinations for monitoring vegetation. *Remote Sensing of Environment*, 8, 127–150.
- Tucker, C. J., & Sellers, P. J. (1986). Satellite remote sensing of primary production. *International Journal of Remote Sensing*, 7, 1395–1416.
- van Leeuwen, W., Hartfield, K., Miranda, M., & Meza, F. (2013). Trends and ENSO/AAO driven variability in NDVI derived productivity and phenology alongside the Andes mountains. *Remote Sensing*, 5, 1177–1203.
- van Leeuwen, W. J. D., Davison, J. E., Casady, G. M., & Marsh, S. E. (2010). Phenological characterization of desert sky island vegetation communities with remotely sensed and climate time series data. *Remote Sensing*, 2, 388–415.
- van Vuuren, D. P., Edmonds, J., Kainuma, M., Riahi, K., Thomson, A., Hibbard, K., Hurtt, G. C., Kram, T., Krey, V., Lamarque, J.-F., Masui, T., Meinshausen, M., Nakicenovic, N., Smith, S. J., & Rose, S. K. (2011). The representative concentration pathways: an overview. *Climatic Change*, 109, 5–31.
- Verbist, K., Santibañez, F., Gabriels, D., & Soto, G., 2010. ATLAS de Zonas Áridas de América Latina y el Caribe. Documento Técnico del PHI-LAC, (25), 48.
- Vicuña, S., Garreaud, R. D., & McPhee, J. (2011). Climate change impacts on the hydrology of a snowmelt driven basin in semi-arid Chile. *Climatic Change*, 105, 469–488.
- Wang, C., Cao, R., Chen, J., Rao, Y., & Tang, Y. (2015). Temperature sensitivity of spring vegetation phenology correlates to within-spring warming speed over the northern hemisphere. *Ecological Indicators*, 50, 62–68.